

Charge storage in doped poly(thiophene): Optical and electrochemical studies

T.-C. Chung, J. H. Kaufman, A. J. Heeger, and F. Wudl

Institute for Polymers and Organic Solids, University of California, Santa Barbara, California 93106

(Received 6 December 1983)

We present a new method of electrochemical polymerization of poly(thiophene) using dithiophene as the starting material, from which we obtain a high-quality film with a sharp interband absorption edge. An *in situ* study of the absorption spectrum during the electrochemical doping process has been carried out. In the dilute regime, the results are in detailed agreement with charge storage via bipolarons; weakly confined soliton pairs with confinement parameter $\gamma \cong 0.1-0.2$. At the highest doping levels, the data are characteristic of the free-carrier absorption expected for a metal. From a parallel electrochemical voltage spectroscopy study, we find evidence of charge injection near the band edge and charge removal from the bipolaron gap states. In the dilute regime, the position of the chemical potential is consistent with charge storage in weakly confined bipolarons. The high Coulombic recovery over a charge-discharge cycle indicates that poly(thiophene) may be an excellent cathode-active material in battery applications.

I. INTRODUCTION

The emergence of organic conducting polymers as a new class of electronic materials has attracted considerable attention. In part, the interest in these materials is based on the premise that through chemical synthesis of new polymers, it should be possible to achieve both chemical stability and a wide range of electronic properties.

The poly(heterocycles) with chemical structure shown in Fig. 1(a) are particularly interesting in this context. In this paper we focus on the electrochemical preparation of polythiophene and the investigation of its optical and electrochemical properties during doping. Polythiophene (PT) can be viewed as an sp^2p_z carbon chain in a structure somewhat analogous to that of *cis*-(CH)_x, but stabilized in that structure by the sulfur, which covalently bonds to neighboring carbons to form the heterocycle. The sulfur may also increase the interchain coupling through *d*-orbital overlap and thereby improve the interchain electron transfer necessary for conductivity. After *p* doping, polythiophene is relatively stable in air, due at least in part to the resonance effect of the sulfur which acts to stabilize a carbonium ion on the polymer chain.

Polymers such as poly(thiophene) are of current theoretical interest since the two structures sketched in Fig. 1(b) are not energetically equivalent. Thus, the cou-

pling of electronic excitations to chain distortions (inherent in such linear conjugated polymers) will lead to polarons and bipolarons as the dominant charged species.¹⁻⁴

The preparation of polythiophene has been reported by several groups, using either electrochemical or chemical synthetic methods.⁵ Chemical preparation of polythiophene typically involved the polycondensation of 2,5-dibromothiophene using a nickel catalyst. Because of the difficulty in purification of 2,5-dibromothiophene, the resulting polymer has a relatively low electronic conductivity ($\sim 10^{-4} \Omega^{-1} \text{cm}^{-1}$) after I₂ doping. Recently, stereoregular PT of relatively high quality has been prepared using 2,5-diiodothiophene.⁶ X-ray powder patterns have demonstrated that the chemically synthesized PT is crystalline.⁷ After doping this material with AsF₅ (~ 24 mol %), the electrical conductivity increased by nearly 10 orders of magnitude to $14 \Omega^{-1} \text{cm}^{-1}$; the magnitude and temperature dependence of the thermopower are consistent with metallic behavior.⁶

Electrochemically polymerized poly(thiophene) has been prepared by several groups.⁸ In these studies, the polymerization step was carried out at relatively high applied voltages, which may cause decomposition of the electrolyte solution and hence may terminate the polymerization process at low molecular weights. Long-range chemical structural order cannot be achieved under such conditions, since the polymerization can also proceed through the β -carbons. Such conditions will destroy the straight-chain geometry and will limit the electronic conjugation. Nevertheless, relatively high electrical conductivities have been reported⁸ for electrochemically synthesized films; $\sigma \sim 100 \Omega^{-1} \text{cm}^{-1}$ was obtained at dopant concentrations of ~ 33 mol % (ClO₄⁻).

In this paper, we present a new method of electrochemical polymerization of PT using milder conditions and dithiophene as the starting material.^{8(a)} We obtain a high-quality film with a sharp interband absorption edge. An *in situ* study of the absorption spectrum during the electrochemical doping process and as a function of the

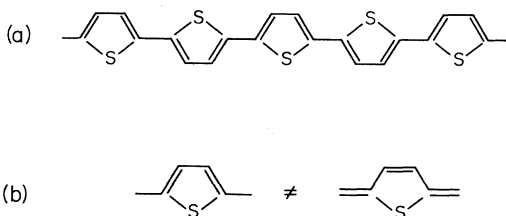


FIG. 1. (a) Chemical-structure diagram of poly(thiophene). (b) Two inequivalent structures for the thiophene heterocycle in poly(thiophene).

dopant concentration has been carried out for doped polythiophene, $[T^{+y}(\text{ClO}_4^-)_y]$, where T designates the thiophene ring [see Fig. 1(a)]. In the dilute regime, the results are in agreement with charge storage in bipolarons (confined soliton pair). As the polythiophene was doped from $y=0$ to $y=0.2$, two absorption features appeared within the gap and grew in intensity with increased dopant concentration, while the interband absorption peak decreased in intensity. At the highest doping levels, $y > 0.2$, the data are characteristic of the free-carrier absorption expected for a metal. This is the first spectroscopic observation of a metallic state (with no remnant of the semiconductor interband transition) in the material with a nondegenerate ground state. From a parallel electrochemical-voltage-spectroscopy (EVS) study of polythiophene, we find the threshold voltage for p -type charge injection to be consistent with the spectroscopic results. The high Columbic recovery over a charge-discharge cycle indicates that polythiophene may be an excellent cathode-active material in battery applications.

II. EXPERIMENTAL TECHNIQUES

The reagents and solvents used in this research were carefully purified as described below:

(i) Dithiophene was recrystallized from methanol four times. This material was then pumped in vacuum for 30 min at 40°C in a storage vessel before transferring to the dry box.

(ii) Thiophene was decolorized with charcoal and was distilled into a storage vessel under a nitrogen flow. Additional vacuum distillation was carried out before use.

(iii) Acetonitrile was dried with P_2O_5 powder, degassed, and vacuum-distilled before use.

(iv) Propylene carbonate was vacuum-distilled into a storage vessel and was stored in a dry box together with some pure lithium metal in order to continuously remove traces of water, dissolved air, etc.

(v) Anhydrous LiClO_4 was pumped for approximately 30 min, and while pumping, was heated gently with a smoky flame. This was done until the LiClO_4 had melted. The LiClO_4 was allowed to cool to room temperature before use.

(vi) A lithium ribbon was cut from commercially available foil, in the dry box, and the oxides were removed mechanically from its surface by scraping with a knife.

In order to be able to prepare high-quality poly(thiophene), a special electrochemical cell was designed and constructed to provide an oxygen- and water-free environment during the electrochemical polymerization process. A schematic diagram of the cell is shown in Fig. 2. The glass cell consisted of a completely sealed single-arm system with two parallel electrodes: an aluminum electrode and a substrate electrode. The substrates used were platinum foil (for EVS studies) or conducting glass (for optical studies). The upper edges of the substrates were kept free of electrolyte solution and were notched so that a Pt wire could be wrapped around to make a good pressure contact to the conducting surface. To minimize the internal resistance of the cell, the distance between two electrodes was made as small as possi-

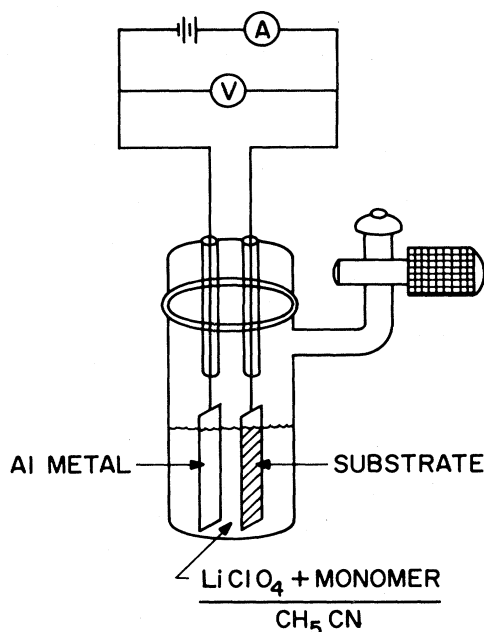


FIG. 2. Diagram of apparatus used for electrochemical polymerization of dithiophene.

ble, ~ 3 mm. The electrolyte solution ($0.5M$ LiClO_4 in acetonitrile with $0.1M$ monomer, dithiophene or thiophene) filled the region between the two electrodes, completing the internal circuit.

After evacuating the cell, it was transferred into the dry box. The substrate working electrode was then attached to the positive terminal of a constant-current power supply through an ammeter; the Al counterelectrode was connected to the negative terminal. A voltmeter, connected between the electrodes, was used to measure the potential difference between them. A constant current of 0.5 mA/cm^2 was applied across the cell. The voltage across the two electrodes was kept relatively small. For dithiophene, the initial voltage was 3.8 V (versus Li) dropping to 3.6 V (versus Li) where most of the polymerization was carried out. For thiophene, the initial voltage was 4.8 V dropping to about 4.5 V. A typical example is shown in Fig. 3. The substrate surface quickly becomes covered by a conducting PT film, which continues to grow in thickness as the polymerization proceeds. The polymerization time is about 2 min to grow a semitransparent film for optical measurements and about 1 h to

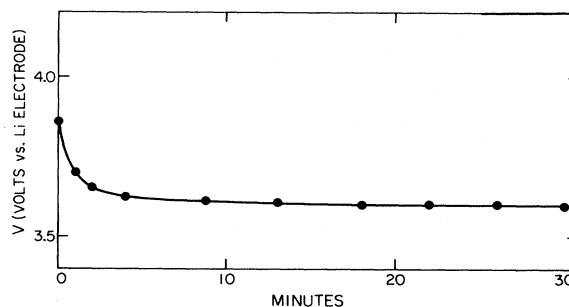
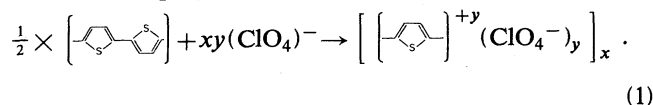
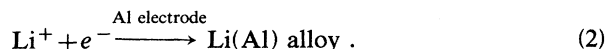


FIG. 3. $V(t)$ during electrochemical polymerization of dithiophene at a constant current of 0.05 mA/cm^2 .

grow a thicker film suitable for the EVS measurement. The reaction at the anode involves simultaneous polymerization and doping:



The corresponding reaction at the cathode is



Thus, the cathode reaction is clean and does not generate decomposition products during the polymerization reaction. The electrolyte solutions remain clear and colorless throughout the electrochemical synthesis.

The spectroscopy of the *as-grown* films is indicative of the doping level achieved during the polymerization reaction [see Eq. (1)]. Polymerization of thiophene (4.5–4.8 V) yields a spectrum characteristic of a heavily doped metallic state, whereas polymerization of dithiophene at the lower applied voltage (3.6–3.8 V) results in a spectrum characteristic of intermediate doping levels (see Sec. III for spectra at doping levels corresponding to these applied voltages). In either case, the (blue-black) film can be undoped back to a neutral (red) state (see Sec. III) with a spectrum essentially identical to that of pure polythiophene prepared by direct chemical coupling. In this paper we focus exclusively on PT films prepared electrochemically with the voltage profile of Fig. 3 using dithiophene starting material.

III. *in situ* SPECTROSCOPY (VISIBLE-TO-NEAR IR) OF POLYTHIOPHENE

A Pyrex cell was designed and constructed so that the visible to near ir spectra of polythiophene could be recorded *in situ* throughout the electrochemical doping and/or undoping process. A schematic diagram is shown in Fig. 4; the glass cell consists of two arms joined at the bottom

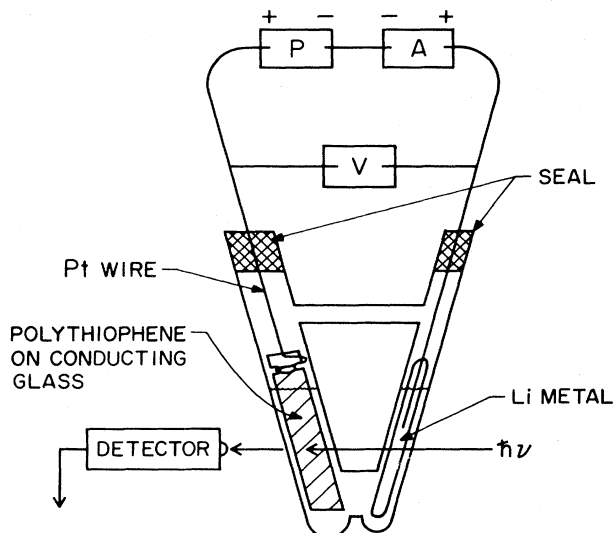


FIG. 4. Diagram of apparatus used for *in situ* visible-ir-absorption measurements during electrochemical doping.

containing a lithium-metal strip in one arm and the polythiophene sample on conducting glass in the other arm. The electrolytic solution, 0.5M LiClO₄ in propylene carbonate, extended into both arms, completing the internal circuit. The arm of the cell which contained the polythiophene film was constructed of rectangular tubing in order to minimize scattered light, to prevent divergence of the beam, and to minimize the ratio of the electrolyte to polythiophene volumes. To maintain long-term stability of the cell, both arms were carefully sealed, with the wire contacts extending through the seals. Another identical cell containing the conducting glass, electrolyte, etc., but with no polymer film, was used as a reference for determining the absorption background.

Absorption measurements were made utilizing a McPherson EU700 monochromator and an IR Industries Si/PbS two-color detector and photomultiplier using standard light-chopping and lock-in-amplifier techniques. The monochromator and lock-in amplifier were interfaced to an Analog Devices MacSym II minicomputer for data acquisition and analysis. In a typical experiment, the reference cell was run first to obtain an effective "source" spectrum I_0 involving all absorptions not due to the polythiophene. The data were stored in the MacSym II. The cell containing the polythiophene was then rigidly mounted in the light path so that a single area was in the beam throughout the doping-undoping cycle, thus allowing quantitative *in situ* comparison of the spectra for each voltage (i.e., each dopant concentration). The raw transmission data (I_t) as well as the optical density [$-\ln(I_t/I_0)$] were stored in the computer for each value of the applied voltage. The voltage across the cell was then changed to the next desired value, and the cell was allowed to come to equilibrium. During this time, the monochromator was set at 2.5 eV, and the strength of the band-gap transition $\alpha(\omega)$ was monitored by the computer along with the cell current. Initially, after stepping the external voltage, current flows and then decays steadily with time as the cell approaches equilibrium. Typical current levels were $\sim 10^4$ nA after a voltage step falling to about 10 nA as the cell approaches diffusion equilibrium with a time constant of about 0.5 h. Correspondingly, the absorption coefficient at 2.5 eV changes continuously after a voltage step and approaches a steady value characteristic of the new dopant concentration. After these parameters had reached steady state, a spectrum was taken. The data were analyzed in terms of the optical density or absorption coefficient, $\alpha = (1/d)\ln(I_t/I_0)$. The film thickness (d) was estimated in the following manner. Under constant-current conditions (0.5 mA/cm²), a 3-cm² film prepared for EVS measurements (see Sec. IV) grew to a mass of 1.8 mg (removed from the substrate and weighed) in 1 h. Thus, in 2 min of film growth (assuming linearity with time under constant-current growth) the mass is 6×10^{-5} g. Using the density of poly(thiophene), 1.4 g/cm³, we find $d \cong 1500$ Å.

As shown in the preceding section, after electrochemical polymerization PT is in the doped state (oxidized). By subsequently lowering the cell voltage, the polymer film can be undoped back to neutral. The neutral point was determined directly from the spectroscopic data; with 2.5

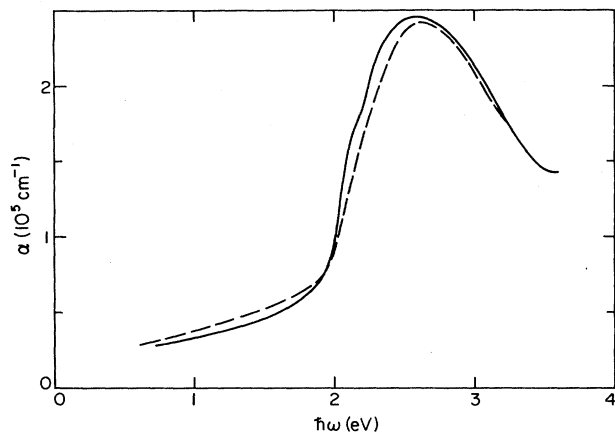


FIG. 5. Absorption coefficient of neutral polythiophene: The solid curve was obtained from an electrochemically synthesized film; the dashed curve was obtained from chemically synthesized material.

V applied the spectrum is essentially identical to that obtained from chemically synthesized pure PT (Ref. 6) (Fig. 5). Thus 2.5 V versus Li corresponds to the neutral point ($y=0$) for polythiophene. The frequency-dependent absorption of neutral poly(thiophene) is that of a semiconductor with an energy gap (as determined by the onset of the π - π^* transition) of about 2 eV.⁶

Figure 6 shows a series of absorption spectra taken during the doping cycle at different applied voltages (y in mol % per thiophening): 3.6 V ($y=2.8$), 3.65 V ($y=4$), 3.7 V ($y=5.4$), 3.8 V ($y=9.6$), 3.85 V ($y=12$), 3.9 V ($y=14$), and 4.05 V ($y=20$). In each case the cell was allowed to come to quasiequilibrium before taking the spectra. Doping levels were obtained from direct electro-

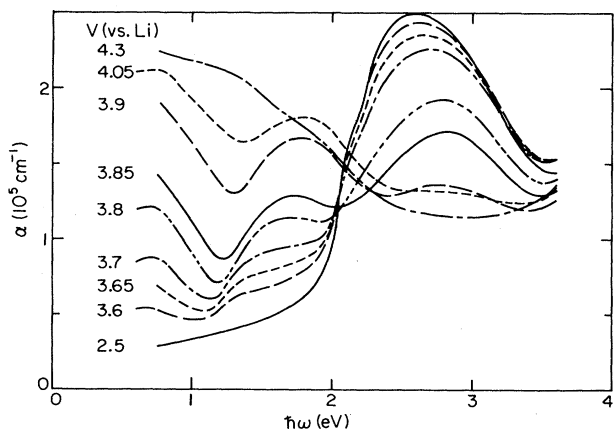
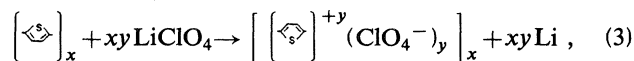


FIG. 6. *In situ* absorption curves for polythiophene during electrochemical doping with $(\text{ClO}_4)^-$. The applied voltages (vs Li) are shown on the left. The corresponding concentrations were obtained from EVS measurements (see Sec. IV) and are as follows (in mol % per thiophene ring): $V_{\text{app}}=3.60$ V, $y=2.8\%$, $V_{\text{app}}=3.65$ V, $y=4\%$, $V_{\text{app}}=3.70$ V, $y=5.4\%$, $V_{\text{app}}=3.80$ V, $y=9.6\%$, $V_{\text{app}}=3.85$ V, $y=12\%$, $V_{\text{app}}=3.90$ V, $y=14\%$, $V_{\text{app}}=4.05$ V, $y=20\%$.

chemical measurements for V_{app} versus Q in a parallel experiment using electrochemical voltage spectroscopy (see Sec. IV).

As the doping proceeded via the oxidation reaction,



the intensity of the interband transition decreased continuously and the absorption peak shifted toward higher energy. In addition, two new absorption features appeared in the ir below the gap edge with intensities which increased as the dopant level increased. The lower-energy ir peak remains at a constant energy (~ 0.65 eV), while the higher-energy one shifts toward higher energy as the dopant level is increased. At 4.3 V, the frequency-dependent absorption is characteristic of the free-carrier spectrum of the metallic state, similar to that found in heavily doped (either chemically or electrochemically) polyacetylene.⁹⁻¹¹

The spectra of Fig. 6 for $h\omega > 0.8$ eV were obtained using an identical cell (but with no sample) as reference. However, below 0.8 eV the strong absorption of the electrolyte solution limited the accuracy of the data. The extension of the curves on Fig. 6 below 0.8 eV was carried out on selected individual samples which were doped (to a particular applied voltage) and sealed in a tube without solution.

Better accuracy was obtained by analyzing the difference spectra from the sample. Two examples are shown in Figs. 7(a) ($V_{\text{app}}=3.65$ V, $y=1$ mol % per carbon) and 7(b) (3.85 V, $y=3$ mol % per carbon). In each case the spectrum was taken at the appropriate applied-cell voltage (versus Li), and the neutral-point spectrum (2.5 V, $y=0$ mol %) was used as the reference. The two dopant-

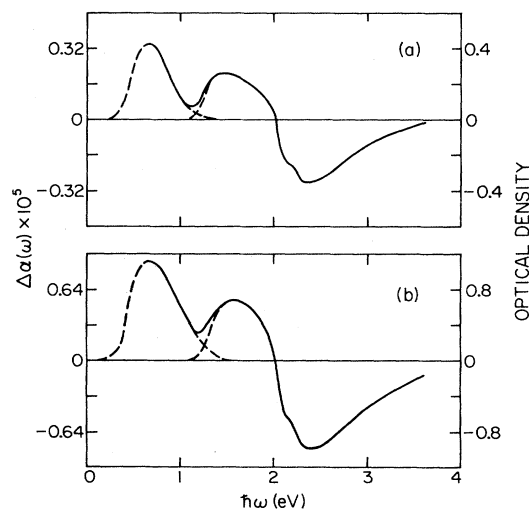


FIG. 7. Difference spectra obtained from the data of Fig. 6. (a) $V_{\text{app}}=3.65$ V, $y=4$ mol % (or 1 mol % per carbon). (b) $V_{\text{app}}=3.85$ V, $y=12$ mol % (or 3 mol % per carbon). In each case the neutral-point spectrum ($V_{\text{app}}=2.50$ V) was used as the reference. The dashed curves are extrapolations which attempt to separate the contributions from the two absorption peaks (see text).

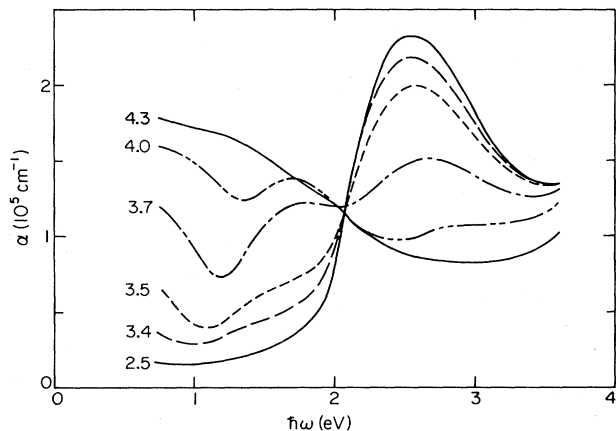


FIG. 8. *In situ* absorption curves for poly(thiophene) during the undoping part of the cycle. The voltages (vs Li) are shown on the left.

induced infrared bands are seen clearly with peaks at $\hbar\omega_1=0.65$ eV and $\hbar\omega_2=1.5$ eV. As noted above, $\hbar\omega_1$ is essentially independent of dopant concentration, whereas $\hbar\omega_2$ increases with increasing frequency. Examination of Figs. 6 and 7 indicates that the oscillator strength of these two dopant-induced ir absorption bands is comparable to that of the midgap absorption in polyacetylene.^{11,12} We conclude, therefore, that these two absorption features arise from electronic transitions between the valence band and two localized energy levels which appear in the gap upon charge-transfer doping.

The difference spectra of Fig. 7 show that the oscillator strength which appears below the gap edge comes primarily from the interband transition. In contrast to *trans*-polyacetylene,^{11,12} the loss of interband oscillator strength is not uniform, but is greatest for frequencies near the band edge.

A procedure similar to that described above was carried out in the subsequent electrochemical undoping process by using a series of stepped-down constant applied potentials. In Fig. 8, spectra 1–6, from top to bottom, were obtained at the designated voltage values. The electrochemical reaction is the reverse of Eq. (3). At $V_{app}=2.5$ V, the spectrum of undoped polythiophene was reproduced.

We note that both on the doping and undoping parts of the cycle, an isosbestic point appears at $\hbar\omega=2.0$ eV for dilute doping levels. At higher dopant concentrations (e.g., for $V_{app}>3.85$ V, $y>3$ mol% per carbon) this isosbestic point disappears and the spectrum qualitatively changes, evolving toward that of the metallic limit.

IV. ELECTROCHEMICAL VOLTAGE SPECTROSCOPY OF POLYTHIOPHENE

Electrochemical voltage spectroscopy is a unique method of determining the energies of charge injection and removal as well as the kinetics of these processes.^{13–16} The technique is basically computer-controlled chronoamperometry and was developed by Thompson¹³ as a method for precise V -versus- Q measurements of an electrochemical cell at quasiequilibrium.

The electrochemical cell employed in this study is constructed by sandwiching a separator (glass filter paper) between a polythiophene-film electrode and lithium electrode, squeezing the assembly into rectangular glass tubing (3×9 mm²), adding the electrolyte solution (0.5M LiClO₄ in propylene carbonate), and sealing the tube under vacuum with both wires extending through the seal. By this method of construction, the minimum amount of electrolyte was employed, air was excluded and the electrodes were held firmly and separated by a very short distance, ~ 0.5 mm, from each other.

The polythiophene electrode was prepared in the doped state as described in Sec. II (size: 3 cm², 1.8 mg). The open-circuit voltage (after polymerization) is $V_{OC}=3.6$ V (versus Li). The cell is then displaced from equilibrium by a small potential step, $\Delta V=0.05$ V, and the current through the cell is monitored via an ammeter. When the current falls below a designated value (sufficiently small to assure quasiequilibrium), the current is integrated, yielding the charge ΔQ that flowed on the decreasing cell voltage from V_0 to $V_0-\Delta V$. This process was repeated until the cell voltage 2.5 V was reached. A similar procedure was used in the charging cycle. Figure 9 shows the V -versus- Q data for PT versus Li. The data were taken at $I_{min}\cong 2$ μ A/mg, with voltage steps $\Delta V\cong 0.02$ V over the range $2.5 < V_{ext} < 3.8$ V. The corresponding dopant level varied from 0 at the neutral point ($\cong 2.5$ V versus Li) to a maximum of about 20 mol% (per thiophene ring), or about 4.0 mol% per carbon. An injection threshold is observed at $\cong (3.45\pm 0.05)$ V versus Li. Hysteresis is evident; final charge removal occurs at 3.15 V. The inset shows dQ/dV versus V for the same cycle. The charge-injection and -removal peaks are clearly evident.

The oxidation levels, given as y (in mol% per thiophene ring) are shown in Fig. 10 for different applied potentials upon charging. To obtain the corresponding concentrations on a per carbon basis, one must simply divide by 4. These are three points to be emphasized.

(i) Since each dopant ion carries unit charge knowledge of V_{app} versus Q is equivalent to knowledge of V_{app} versus y . The y values in Fig. 10 were obtained in this way.

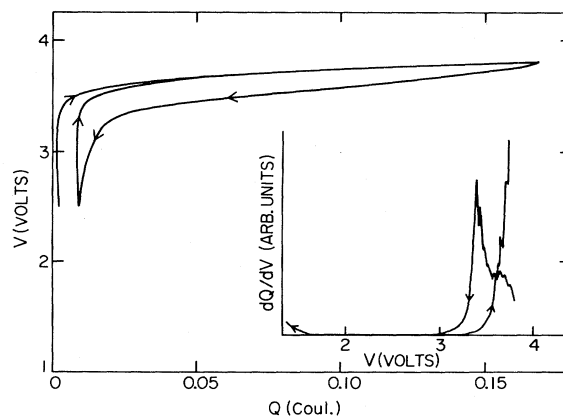


FIG. 9. V vs Q (in coulombs) for polythiophene vs Li; the inset shows dQ/dV vs V for the same cycle.

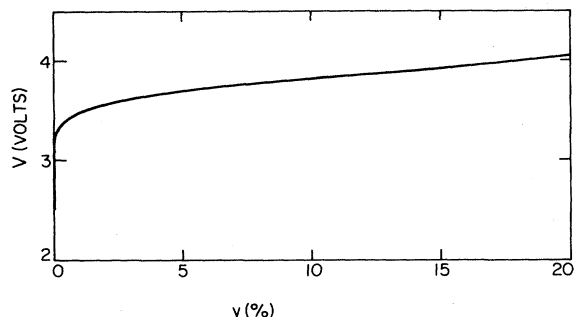


FIG. 10. V vs y in mol% for $[T^{+y}(\text{ClO}_4^-)_y]_x$ where T denotes the thiophene heterocycle. The data were obtained using EVS, on charging, and used a Li reference electrode.

(ii) The Coulomb efficiency is extremely high in this system, $Q_{\text{out}}/Q_{\text{in}}=97\%$ upon charging from 2.5 to 3.8 V (versus Li) and $Q_{\text{out}}/Q_{\text{in}}=87\%$ upon charging to 4.05 V (versus Li). Therefore, the calculated dopant concentrations using Q_{in} or Q_{out} are not significantly different.

(iii) The difference between V_{app} and V_{OC} is very small since the measurement at each charging step is carried out under quasiequilibrium conditions.

V. DISCUSSION AND ANALYSIS OF RESULTS: BIPOLARONS IN DOPED POLYTHIOPHENE

The absorption spectrum of neutral polythiophene is remarkably similar to that of *trans*-(CH)_x,^{11,12} but is blue-shifted by about 0.4–0.5 eV. Even the familiar structure on the leading edge, attributed by Melé to dynamical chain distortion following electron-hole-pair creation,¹⁷

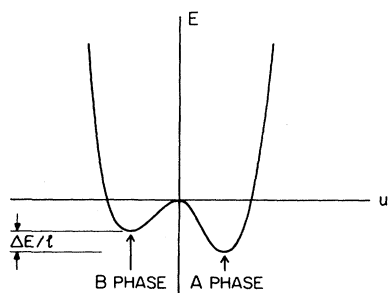
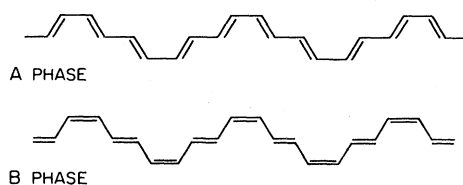


FIG. 11. Schematic diagram of poly(thiophene) backbone structure leaving out the sulfur atoms (see Fig. 1). The two configurations (*A* and *B* phase) are nearly (but not precisely) degenerate as shown in the diagram at the bottom of the figure where we plot energy versus the distortion parameter u ($u=0$ when the bond lengths are equal).

is evident in the data. These similarities suggest that polythiophene can be viewed as being similar to *trans*-(CH)_x, but with the ground-state degeneracy lifted by a small amount due to the inequivalence of the two structures with opposite bond alternation. We emphasize the analogy between PT and (CH)_x in the diagrams of Fig. 11 where we redraw the polythiophene backbone structure, purposely leaving out the sulfur heteroatom. The resulting structure is that of an sp^2p_z polyene chain consisting of four carbon all-*trans* segments linked through a *cis*-like unit. In such a structure the ground state is not degenerate (as in Fig. 11). However, the energy difference per bond, $\Delta E/l$, might be expected to be small; i.e., greater than 0 [as in *trans*-(CH)_x] but less than that of *cis*-(CH)_x. An obvious consequence of the lack of degeneracy is that the schematic PT structure of Fig. 11 cannot support stable soliton excitations,¹⁻⁴ since creating a soliton pair separated by a distance d would cost energy $\sim d(\Delta E/l)$. This linear "confinement" energy leads to bipolarons as the lowest-energy charge-transfer configurations in such a chain.

Although this description of PT is admittedly schematic, there is experimental evidence that it represents an excellent starting point for a more detailed description of the doping processes in this system. The optical-absorption data (Figs. 6–8) indicate an energy-level structure at dilute doping levels as shown in Fig. 12 with $\hbar\omega_1 \cong 0.60-0.65$ eV and $\hbar\omega_2 \cong 1.4-1.45$ eV. We use values for $\hbar\omega_1$ and $\hbar\omega_2$ just below the peaks since the transitions involved are between a localized gap state and the valence-band density of states. The value for the interband absorption can be estimated from the data of Figs. 6–8 to be $\hbar\omega_1 \cong 2.1$ eV. In this case, the joint density of states of the valence and conduction bands is involved in the absorption so that the point of steepest slope in $\alpha(\omega)$ (Fig. 6) or the crossover in the difference curves (Fig. 7) is used. Although there is surely some uncertainty in the assignment of the precise energies, the data from the dilute dopant concentrations yield

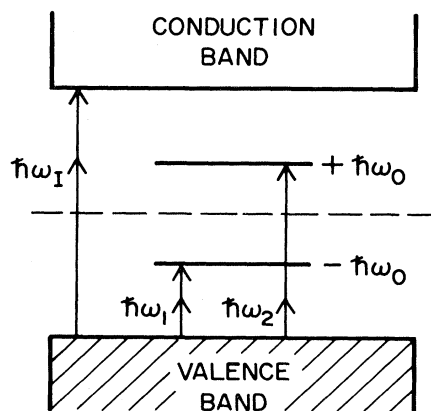


FIG. 12. Energy-level diagram for poly(thiophene) at dilute doping concentrations. The spectroscopic data of Figs. 6 and 7 imply the formation of the empty energy levels symmetric about the gap center.

$$\hbar\omega_1 + \hbar\omega_2 \cong \hbar\omega_1 = E_g, \quad (4)$$

where $E_g \cong 2\Delta_0$ is the energy gap. The results expressed quantitatively in Eq. (4) indicate the existence of electron-hole symmetry in the doped polymer. Referring to Fig. 12, the two doping-induced energy levels appear *symmetrically* with respect to the gap center at $\pm\hbar\omega_0 = (0.40 \pm 0.05)$ eV. The existence of electron-hole symmetry implies that the schematic structure of Fig. 11 represents an essentially correct point of view. The sulfur atoms stabilize the polyene chain in the configuration of Fig. 11 through covalent bonding to neighboring carbon atoms. Evidently, however, the sulfur is only weakly interacting with the π -electron system of the polyene backbone. If this were not the case, some of the transferred charge would reside on the sulfur, and the electron-hole symmetry implied by Figs. 6–8 and sketched in Fig. 9 would not be present.

We assign the two energy-gap states shown in Fig. 12 to the two levels expected from charge storage in bipolaron states in doped PT.^{1–4} This assignment is based on three facts:

(1) The two transitions imply formation of two levels symmetric with respect to the gap center.

(2) The observation of *only* two transitions implies that the two levels are not occupied. If there were electrons in the lower level (as would be the case for a “hole” polaron), then a third absorption would be evident arising as a transition between the two localized levels. This is not observed.

(3) Analysis of the data leads to $\hbar\omega_0/\Delta_0 \cong 0.35$. This small value is inconsistent with polaron formation for which $\hbar\omega_0/\Delta_0 \geq 0.707$.^{1,2}

The small value inferred for $\hbar\omega_0/\Delta_0$ implies weak confinement. Using the results obtained by Fesser, Bishop, and Campbell (FBC)² in their detailed analysis of the bipolaron problem, we can extract values for the relevant microscopic parameters. The confinement parameter is defined as

$$\gamma = \Delta_e / \lambda \Delta_0, \quad (5)$$

where Δ_e is the constant external gap parameter ($2\Delta_e$ would be the energy gap without the bond-alternation contribution, Δ_i , which arises from the spontaneous symmetry breaking due to the Peierls instability), λ is the dimensionless electron-phonon coupling constant appropriate to the twofold commensurate case, and Δ_0 is the full gap parameter ($\Delta_0 = \Delta_e + \Delta_i$). From Fig. 4 of FBC, we obtain $\gamma \cong 0.1–0.2$ using the experimental value for $\hbar\omega_0/\Delta_0 \cong 0.35$. This small value for γ , implying weak confinement, is consistent with the point of view expressed in Fig. 11 and with the remarkable similarity of the shape of the absorption curves of neutral *trans*-(CH)_x and neutral PT. The confinement parameter has been estimated to be $\gamma \sim 0.5–1.0$ for *cis*-(CH)_x.² This large value leads to qualitatively different behavior in the dynamics following *e-h*-pair creation in *cis*-(CH)_x and thereby to the distinctly different features observed on the absorption curve, as shown by Melé.¹⁷

The one-dimensional (1D) energy gap in *trans*-(CH)_x has been estimated as $E_g^{1D} \cong 1.6–1.8$ eV.¹⁸ Taking the

value of $E_g^{1D} \cong 2.1$ eV for polythiophene, we estimate $\Delta_e \cong 0.15–0.2$ eV. Thus from Eq. (5), we find $\lambda \sim 0.5–1$ for PT. Although this is quite clearly not a precise determination of λ , the resulting value is reasonable. Note that even though the sulfur appears to play only a minor role in the π -electron structure of PT, the bonding to neighboring carbons to form the heterocycle may lead to significant contributions to the chain stiffness, phonon dispersion and the electron-phonon coupling constant, etc.

The relative intensities of the two gap absorptions, $\hbar\omega_1$ and $\hbar\omega_2$, can be obtained from Fig. 7. Although the *in situ* configuration does not allow data acquisition at frequencies below about 0.6 eV, the overall features are clear (we have sketched the extrapolated shape of $\hbar\omega_1$ to lower frequencies based on the line shape expected for a transition between a localized state and a 1D band). The lower-energy peak has the greater integrated intensity by about a factor of 2; i.e., $I(\hbar\omega_1)/I(\hbar\omega_2) \cong 2$. This ratio has been calculated by FBC. They find $I(\hbar\omega_1) > I(\hbar\omega_2)$ for bipolarons, in agreement with the experimental results; but with $\hbar\omega_0/\Delta_0 \cong 0.35$ they predict $I(\hbar\omega_1)/I(\hbar\omega_2) \cong 6$. The origin of this discrepancy is not clear. However, it is obvious that the model is oversimplified in many ways. Particularly, in calculating intensities of transitions, where the details of the wave functions are important, such a quantitative discrepancy is not surprising.

In the case where the ground state is degenerate, the midgap transitions “steal” oscillator strength *uniformly* from the interband transition. This has been observed and experimentally verified in the *in situ* optoelectrochemical spectroscopy studies of *trans*-(CH)_x.¹¹ For PT, this is not the case. Figures 6 and 7 demonstrate that as the doping proceeds, the interband transition weakens, but not uniformly. The loss of oscillator strength is greater near the interband edge, causing the apparent shift to higher energies with increasing dopant concentration. Although a detailed quantitative comparison is difficult, FBC have shown (see Fig. 9 of their paper) that the loss of oscillator strength $\beta(\omega)$ is greater near the band edge in the case of bipolarons. Using $\hbar\omega_0/\Delta_0 \cong 0.35$ (appropriate to PT), $\beta(\omega)$ is 2 times greater for $\hbar\omega \cong E_g$ than the corresponding value at higher energies. Thus the qualitative features of the observed changes in interband absorption are in excellent agreement with the predictions based on charge storage in bipolarons. A more detailed analysis is not possible at the present time because of the limited spectral range currently available.

As the dopant concentration is increased, $\hbar\omega_1$ remains essentially constant, whereas $\hbar\omega_2$ shifts toward higher energies. This concentration-dependent shift is not expected within the confines of the noninteracting-bipolaron theory.^{1–4} The shift may signal the importance of interactions between bipolarons, leading, at sufficiently high concentrations, to the metallic state. Alternatively, the shift may imply some involvement of the sulfur heteroatom at high dopant levels, leading to a breakdown of the precise electron-hole symmetry. We note in this context that the electron-spin-resonance line of heavily doped metallic PT (doped with AsF₅) exhibits a small *g* shift (2.008) relative to that of polyacetylene under similar conditions (2.0026), implying that some charge exists on the

sulfur heteroatom at high dopant levels.¹⁹

In the heavily doped limit ($V_{\text{app}}=4.3$ V), all signs of the interband transition have disappeared, and the spectrum (Fig. 6) is dominated by the free-carrier absorption in the infrared. In this regime, the optical properties of doped PT are those of a metal. The magnitude and spectral dependence of $\alpha(\omega)$ are similar to those reported earlier^{9,10} for Na-doped *trans*-(CH)_x where electrical conductivities in excess of $10^3 \Omega^{-1} \text{cm}^{-1}$ were inferred from the frequency-dependent absorption in the ir and subsequently observed directly in dc measurements.¹⁰ Thus, metallic doped PT can be expected to be an excellent conductor. Although previous conductivity measurements on electrochemically synthesized (and doped) PT yielded values as high as $100 \Omega^{-1} \text{cm}^{-1}$,⁸ the intrinsic values may, in fact, be much higher.

The EVS measurements (Figs. 9 and 10) provide complementary information. Charge injection (oxidation) occurs above about (3.45 ± 0.05) V versus Li (see Fig. 9). Since the neutral point is at 2.5 V (versus Li) this charge-injection threshold implies $\Delta_0 \cong (0.95 + 0.05)$ eV. Preliminary attempts at *n*-doping (reducing) the polymer exhibited a threshold at about 1.6 eV, indicating approximate symmetry about the neutral point and an electrochemically determined energy gap of about 1.9 eV. A value slightly smaller than the optical gap is expected since initial injection should occur as a single polaron at an energy of about $0.9\Delta_i$ (in the weak-confinement limit, approaching Δ_0 as γ increases).¹⁶

Hysteresis is observed in the V -versus- Q cycle reminiscent of similar effects reported earlier for polyacetylene.¹⁴⁻¹⁶ A detailed analysis¹⁶ of the many contributions to the free energy has been carried out for polyacetylene, leading to the conclusion that the hysteresis is intrinsic; charge is injected near the band edge, but stored in gap-center states associated with soliton pairs generated by structural relaxation around the injected charges. In poly(thiophene), because the ground state is nondegenerate, the corresponding coupling of the π electron to chain distortions leads to a splitting of the midgap states into the symmetric bipolaron levels and to charge storage in the bipolaron gap states, as demonstrated by the analysis of the visible-ir-absorption data. Thus, in PT, the hysteresis in V versus Q arises from charge injection near the band edge (single polarons), and charge removal from the bipolaron gap states. Note that since bipolarons can exist only in the doubly charged state, removal of a charge will yield a charged polaron. The identification of the maximum in dQ/dV (upon removal) with the bipolaron chemical potential therefore relies on the infrared-absorption data, which show no evidence of single polarons either on the doping or the undoping parts of a cycle. Evidently, the kinetics of the recombination of polaron pairs into lower-energy bipolarons is sufficiently rapid in poly(thiophene) so that no significant polaron population is ever achieved. In the case of poly(pyrrole), where the kinetics are slower, the optical data and the chemical potential for charge removal appear to result from a combination of polarons and bipolarons in the sample.^{20,21}

The magnitude of the hysteresis (ΔV) quantitatively locates the chemical potential of the doped polymer (at di-

lute doping levels),

$$\mu = \Delta_0 - \Delta V,$$

measured with respect to the center of the energy gap. Using $\Delta_0 \cong 1.05$ eV and $\Delta V \cong 0.3$ eV (see Fig. 9), we find $\mu \cong 0.7\Delta_0$. This value is slightly larger than that expected ($\mu = 2\Delta/\pi$) for the degenerate ground-state limit where the confinement parameter is 0.¹⁶ The experimental value is therefore consistent with the weak confinement inferred from analysis of the *in situ* spectroscopy data.

Battery cells have been constructed with PT films grown from dithiophene on platinum foil.²² Throughout the dopant range from 0 to 20 mol % per thiophene ring (~ 4.0 mol % per carbon) we obtained Coulomb efficiencies greater than 95%. Cycle-to-cell potentials greater than 4.0 V yielded better than 85% efficiency at doping levels of > 5.0 mol % per carbon. Thus, without resorting to extraordinary techniques to ensure purity, we have found excellent electrochemical stability. After charging such a cell to an open-circuit voltage of 3.8 V, corresponding to ~ 4.5 mol % doping (per carbon), short-circuit currents of about 20 mA/mg were obtained. At the same concentration, the maximum power density was 2.5×10^4 W/kg, based on the weight of doped polymer and the mass of lithium consumed. EVS cycles up to 4.2 V (~ 6 mol % per carbon) demonstrated an energy density of 140 Wh/kg normalized in the same way. Corresponding values for polyacetylene (versus Li) cells at 6 mol % (per carbon) doping are ~ 25 mA/mg (short-circuit current), $\sim 3 \times 10^4$ W/kg (maximum power density), and ~ 176 Wh/kg (energy density).²³ The latter values are also based on the weight of the doped polymer and the mass of lithium consumed. These numbers are for comparison only; corresponding values for packaged cells would be lower.

VI. CONCLUSIONS

An *in situ* study of the absorption spectrum during electrochemical doping has been carried out on polythiophene films polymerized electrochemically using dithiophene as the starting material. In the dilute regime, the results are in detailed agreement with charge storage in bipolarons; weakly confined soliton pairs with confinement parameters of $\gamma \cong 0.1-0.2$. At the highest doping levels, the visible-ir data are characteristic of the free-carrier absorption expected for a metal.

From a parallel electrochemical-voltage-spectroscopy study, we find evidence of charge injection near the band edge and charge removal for the bipolaron gap states. The high voltages and excellent stability obtained with polythiophene employed as a cathode (versus Li) suggest the construction of an all-polymer battery consisting of a PT cathode and a (CH)_x anode. Such a cell should have an open-circuit voltage of about 2.8 V. The all-polymer construction may lead to power and energy densities (packed) competitive with (or even superior to) conventional lead acid batteries.

Previous studies of polyacetylene have demonstrated that the coupling of electronic excitations to nonlinear conformational changes is an intrinsic and important

feature of conducting polymers.²⁴ Although this coupling and the degenerate ground state lead to the novel soliton excitations in *trans*-(CH)_x, generalization of these concepts and application to the larger class of conjugated polymers has been an obvious goal of the field. The experimental evidence of electron-hole symmetry and weak confinement in polythiophene makes this polymer a nearly ideal example of a model system in which the ground-state degeneracy has been lifted. The study of bipolarons (or confined charged solitons) in poly(thiophene) presented in this paper has demonstrated that the concepts carry

over in detail and that a quantitative understanding of the resulting phenomena is possible even for relatively complex systems.

ACKNOWLEDGMENTS

We thank M. Kobayashi for purification of dithiophene. The *in situ* spectroscopy studies reported here were supported by the U. S. Office of Naval Research. The electrochemical synthesis was supported by a grant from Showa Denko K.K.

- ¹S. A. Brazovskii and N. N. Kirova, Pis'ma Zh. Eksp. Teor. Fiz. **33**, 6 (1981) [JETP Lett. **33**, 4 (1981)].
- ²K. Fesser, A. R. Bishop, and D. K. Campbell, Phys. Rev. B **27**, 4804 (1983).
- ³(a) A. J. Heeger, Comments Solid State Phys. **10**, 53 (1981); (b) L. Lauchlan, S. Etamad, T.-C. Chung, A. J. Heeger, and A. G. MacDiarmid, Phys. Rev. B **24**, 3701 (1981).
- ⁴J. L. Brédas, B. Themans, J. M. Andre, R. R. Chance, D. S. Boudreaux, and R. Silbey, J. Phys. (Paris) **44**, 373 (1983); J. L. Brédas, R. R. Chance, and R. Silbey, Mol. Cryst. Liq. Cryst. **77**, 319 (1981).
- ⁵(a) T. Yamamoto, K. Sanechika, and A. Yamamoto, J. Polym. Sci. Polym. Lett. **18**, 9 (1980); (b) J. W.-P. Lin and L. P. Dudek, J. Polym. Sci. Polym. Chem. Ed. **18**, 2869 (1980).
- ⁶M. Kobayashi, J. Chen, T.-C. Chung, F. Moraes, A. J. Heeger, and F. Wudl, Synth. Met. **9**, 77 (1984).
- ⁷H. Yoshida and N. Toneaki (private communication).
- ⁸(a) P. Pfluger and G. B. Street, J. Chem. Phys. (to be published); (b) A. Diaz, Chem. Scr. **17**, 145 (1981); (c) G. Touillon and F. Garnier, J. Electroanal. Chem. **135**, 173 (1982); (d) C. Kossmehl and G. Chalzithedoron, Makromol. Chem. **2**, 551 (1981); (e) J. Bargon, S. Mohmand, R. J. Waltman, IBM J. Res. Dev. **27**, 330 (1983); (f) K. Kaneto, Y. Kohno, K. Yoshino, and Y. Inuishi, J. Chem. Soc. Chem. Commun. **382** (1983).
- ⁹T.-C. Chung, A. Feldblum, A. J. Heeger, and A. G. MacDiarmid, J. Chem. Phys. **47**, 5504 (1981).
- ¹⁰T.-C. Chung, F. Moraes, J. D. Flood, and A. J. Heeger, Phys. Rev. B **29**, 2341 (1984).
- ¹¹A. Feldblum, J. H. Kaufman, S. Etamad, A. J. Heeger, T.-C. Chung, and A. G. MacDiarmid, Phys. Rev. B **26**, 815 (1982).
- ¹²N. Suzuki, M. Ozaki, A. J. Heeger, and A. G. MacDiarmid, Phys. Rev. Lett. **45**, 1209 (1980).
- ¹³A. H. Thompson, Physica (Utrecht) **99B**, 100 (1980); Phys. Rev. Lett. **40**, 1511 (1978).
- ¹⁴J. H. Kaufman, J. W. Kaufer, A. J. Heeger, R. Kaner, and A. G. MacDiarmid, Phys. Rev. B **26**, 2327 (1982).
- ¹⁵J. H. Kaufman, T.-C. Chung, and A. J. Heeger, Solid State Commun. **47**, 585 (1983).
- ¹⁶J. H. Kaufman, T.-C. Chung, and A. J. Heeger, J. Electrochem. Soc. (to be published).
- ¹⁷E. J. Mele, Synth. Met. (to be published); E. J. Mele, Solid State Commun. **44**, 827 (1982).
- ¹⁸D. Moses, A. Feldblum, E. Ehrenfreund, A. J. Heeger, T.-C. Chung, and A. G. MacDiarmid, Phys. Rev. B **26**, 3361 (1982).
- ¹⁹F. Moraes, D. Davidov, and A. J. Heeger (unpublished).
- ²⁰J. C. Scott, J. L. Bredas, K. Yakushi, P. Pfluger, and G. B. Street, Synth. Met. **9**, 165 (1984).
- ²¹J. H. Kaufman, G. B. Street, and J. C. Scott (unpublished).
- ²²J. H. Kaufman, T.-C. Chung, A. J. Heeger, and F. Wudl (unpublished).
- ²³K. Kaneto, M. Maxfield, D. P. Nairns, A. G. MacDiarmid, and A. J. Heeger, J. Chem. Soc. Faraday Trans. **78**, 3417 (1982).
- ²⁴S. Etamad, A. J. Heeger, and A. G. MacDiarmid, Ann. Rev. Chem. Phys. **33**, 443 (1982).